Dijet production as a centrality trigger for *pp* collisions at CERN LHC

L. Frankfurt,[1] M. Strikman,[2] and C. Weiss[3]
[1]*School of Physics and Astronomy, Tel Aviv University, Tel Aviv, Israel*
[2]*Department of Physics, Pennsylvania State University, University Park, Pennsylvania 16802, USA*
[3]*Institut für Theoretische Physik, Universität Regensburg, D-93053 Regensburg, Germany*
(Received 8 January 2004; published 2 June 2004)

We demonstrate that a trigger on hard dijet production at small rapidities allows us to establish a quantitative distinction between central and peripheral collisions in $\bar{p}p$ and pp collisions at Tevatron and LHC energies. Such a trigger strongly reduces the effective impact parameters as compared to minimum bias events. This happens because the transverse spatial distribution of hard partons ($x \gtrsim 10^{-2}$) in the proton is considerably narrower than that of soft partons, whose collisions dominate the total cross section. In the central collisions selected by the trigger, most of the partons with $x \gtrsim 10^{-2}$ interact with a gluon field whose strength rapidly increases with energy. At LHC (and to some extent already at Tevatron) energies the strength of this interaction approaches the unitarity (''blackbody'') limit. This leads to specific modifications of the final state, such as a higher probability of multijet events at small rapidities, a strong increase of the transverse momenta and depletion of the longitudinal momenta at large rapidities, and the appearance of long-range correlations in rapidity between the forward or backward fragmentation regions. The same pattern is expected for events with production of new heavy particles (Higgs boson, SUSY). Studies of these phenomena would be feasible with the CMS-TOTEM detector setup, and would have considerable impact on the exploration of the physics of strong gluon fields in QCD, as well as the search for new particles at LHC.

DOI: 10.1103/PhysRevD.69.114010 PACS number(s): 12.38.−t, 13.85.−t, 14.80.Bn, 25.75.Nq

I. INTRODUCTION

The differences between peripheral and central collisions play a crucial role in the physics of heavy ion collisions. In *pp* collisions, a similar distinction can be made at the energies of the LHC and the Tevatron. This is possible because of the appearance of two separate transverse distance scales at high energies. On one hand, as predicted by Gribov [1], the essential impact parameters in hadron-hadron collisions increase with the energy. This has been observed, e.g., in numerous experiments in elastic *pp* scattering; see Ref. [2] for a review. On the other hand, the transverse spatial distributions of hard partons (with finite light-cone fraction, x) in the colliding nucleons is only a weak function of x. For the gluon distribution this has been verified experimentally in studies of the t dependence of photoproduction of heavy quarkonia off the nucleon [3]. The two scales allow us to classify *pp* collisions at collider energies. A schematic illustration of this idea is given in Fig. 1. In collisions with large impact parameters there will be essentially no overlap between the hard partons (Fig. 1a). Only partons with $x \ll 10^{-2}$ will overlap with significant probability. These peripheral events constitute a significant (in fact, dominant) part of the total inelastic cross section. The production of high $p_\perp$ jets, however, as well as of heavy particles, will be strongly suppressed. At small impact parameters, however, the distributions of hard partons in the two colliding nucleons will overlap, and the probability of hard interactions will be greatly enhanced (Fig. 1b). This difference between the physics of soft and hard QCD processes (i.e., with x_1, x_2 of the colliding partons $\geqslant 10^{-2}$) gives us an opportunity to distinguish quantitatively between central and peripheral collisions at collider energies.

Specifically, we propose here to use the production of (one or more) hard dijets near zero rapidity as a ''centrality trigger'' for $\bar{p}p$ and pp collisions at Tevatron and LHC energies. At the LHC, such a trigger could be implemented with any of the central detectors. It will lead to a significant enhancement of the production of hadrons at small rapidities and drastic changes of the pattern of forward production, which could be probed, for example, by the TOTEM detector in combination with the CMS detector. Since the production of heavy particles, such as the Higgs boson or supersymmetric particles, is also greatly enhanced for central collisions, such a program could have considerable impact on the searches for new particles at the LHC.

Another important application of the proposed ''centrality

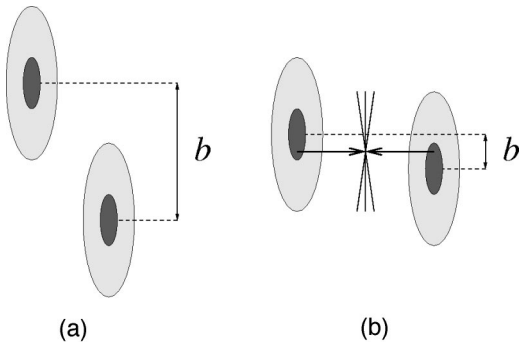

FIG. 1. Schematic illustration of the two classes of *pp* collisions at high energies. The transverse spatial distributions of the hard partons ($x \geqslant 10^{-2}$) is indicated by the dark shaded disks, those of the soft partons ($x \ll 10^{-2}$) by the light shaded disks; b denotes the impact parameter of the *pp* collision. (a) At large b no overlap between hard partons occurs. (b) At small b the distributions of hard partons overlap, leading to production of hard dijets (and, possibly, heavy particles).

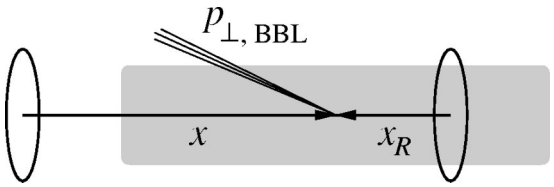

FIG. 2. Schematic illustration of the effect of the black-body (unitarity) limit on hadron production in the forward or backward rapidity region in central *pp* collisions. A small-x spectator parton (i.e., a parton not involved in the centrality trigger) from the left proton propagates through the strong gluon field (indicated by the shaded area), acquiring a large transverse momentum, $p_{\perp,\mathrm{BBL}} \gg \Lambda_{\mathrm{QCD}}$. The small-$x$ parton is then resolved in a collision with a large-x_R parton from the right proton, resulting in hadron production in the backward rapidity region.

trigger'' is in the investigation of the physics of strong gluon fields in QCD. Numerous measurements of small-x phenomena at HERA have confirmed the fast increase of the gluon density in the proton predicted by perturbative QCD; for a review and references see Ref. [4]. At LHC energies, and to some extent already at the Tevatron, the gluon density becomes so large that the interaction of high $p_\perp$ partons with the gluon ''medium'' becomes strong and multiple scattering effects cannot be neglected, for a review and references see Ref. [5]. The new phenomenon one encounters here can be described as the breakdown of the Dokshitzer-Gribov-Lipatov-Altarelli-Parisi (DGLAP) approximation caused by the approach to the unitarity limit [blackbody limit (BBL)], in which partons with virtualities below a certain value interact with the other proton with the maximal strength allowed by *s*-channel unitarity. More quantitatively, a parton in one proton with longitudinal momentum fraction x_R and virtuality $p_\perp^2$ resolves partons in the other proton with

$$x = \frac{4p_\perp^2}{x_R s}, \tag{1}$$

where s is the invariant energy squared of the *pp* collision; see Fig. 2. In particular, large-x_R partons resolve small-x partons in the other proton. At the LHC energy, $\sqrt{s} = 14000$ GeV, for $p_\perp \sim 2$ GeV/c and $x_R \sim 10^{-2}$ one obtains $x \sim 10^{-5}$. Under this condition the interactions with gluons can approach the BBL, see Ref. [5] and references therein. Present data on heavy quarkonium photoproduction indicate that the gluon density at small x is maximum in the transverse center of the proton [3]. Since the distribution of large-x_R partons is likewise concentrated at small transverse distances, it is evident that the chances of approaching the BBL are maximum for central *pp* collisions, which can be selected with the proposed ''centrality trigger.''

The approach to the BBL in central *pp* collisions leads to a significant change of the initial and final state interactions in the hard QCD processes. The interactions with the ''high density gluon medium'' suppress the spectrum of low transverse momentum partons and enhance the high momentum tail. Typically, all partons which are not involved in the hard interactions at the scale much higher than the BBL scale, $p_{\perp,\mathrm{BBL}}$, receive transverse momenta $\sim p_{\perp,\mathrm{BBL}}$ and experience a significant momentum loss due to the gluon radiation (a schematic illustration is provided in Fig. 2). A forward would-be spectator component of the proton wave function is ''pulverized'' completely, loosing its coherence. As a result the number of particles with $x_F \geqslant 0.1$ in the proton fragmentation region will strongly diminish, while the average transverse momenta of these particles will grow to values comparable to $p_{\perp,\mathrm{BBL}}$. Much more energy will be released at small rapidities as compared to minimal bias events.

Although the phenomena discussed here are higher-twist corrections to the inclusive cross section and the transverse spectra of the production of sufficiently heavy particles (Higgs, SUSY), in the vicinity of the BBL they will strongly modify the overall structure of the final states. In particular, they will change the pattern of radiation of moderate $p_\perp$ jets and the Sudakov form factors for dijet production. Thus the understanding of these phenomena is important also for effective searches for new physics at the LHC.

The basic idea of the proposed ''centrality trigger'' is that the restriction to events with production of a hard dijet strongly reduces the effective impact parameters in high-energy $p\bar{p}$ and *pp* collisions as compared to minimum bias events. One can further narrow the distribution of impact parameters by requiring the presence of multiple dijets in the same event (this was first studied within the framework of a multiple interaction Monte Carlo model in Ref. [6]). The actual reduction which can be achieved in this way depends, to some extent, on possible spatial correlations of hard partons in the transverse plane. In this respect we make a surprising observation, namely that the data on double dijet production in $p\bar{p}$ collisions at the Tevatron obtained by the CDF Collaboration [7] indicate significant spatial correlations of partons in the transverse plane.

The paper is organized as follows. In Sec. II we review the available information on the impact parameter distribution in the generic inelastic *pp* collisions. In Sec. III we summarize our knowledge of the transverse spatial distribution of hard partons in the nucleon and study its dependence on the resolution scale. In Sec. IV we calculate the impact parameter distribution in *pp* collisions with production of a hard dijet near zero rapidity, and compare it with the impact parameter distribution for generic inelastic collisions. We demonstrate that hard dijet production acts as a ''centrality trigger.'' We also discuss the extension to production of multiple dijets and the role of possible correlations in the transverse spatial distribution of gluons. In Sec. V we investigate the role of the ''centrality trigger'' in approaching the BBL in central *pp* collisions. We show that the trigger essentially eliminates collisions at large impact parameters where the soft interactions are not black. In Sec. VI we list the novel characteristics of the final state in central *pp* collisions which follow from the proximity to the BBL of the spectator parton interactions at small transverse distances. Our conclusions are presented in Sec. VII.

II. IMPACT PARAMETER DISTRIBUTION FOR GENERIC INELASTIC *pp* COLLISIONS

We begin by summarizing the available information about the impact parameter distribution of the cross section for

generic inelastic *pp* collisions at high energies. Most of our knowledge here comes from *pp* elastic scattering, which has been studied in numerous experiments, see Ref. [2] for a review. By unitarity (i.e., the optical theorem) the *pp* elastic amplitude contains information also about the total (elastic plus inelastic) cross section, and thus about the inelastic cross section.

It is well known from studies of *pp* elastic scattering that the radius of strong interactions (the average impact parameter) increases with the collision energy, s. The t slope of the elastic cross section, B, grows as

$$B(s)=B(s_0)+2\alpha'\ln(s/s_0), \tag{2}$$

with $\alpha'\approx 0.25\ \mathrm{GeV}^{-2}$. Thus, the radius of strong interactions is expected to be a factor of 1.5 larger at LHC as compared to fixed target energies.

In the partonic picture, the mechanism for the increase of the radius of strong interactions with energy is the so-called Gribov diffusion. The emission processes in the soft parton ladder give rise to a random walk of partons in the transverse plane, reminiscent of a diffusion process [8]. If one writes the amplitude of elastic scattering of two hadrons as a product of two t-dependent form factors, each parameterized by the transverse radius of the hadron, R,

$$A^{h_1h_2}\propto\exp(tR_1^2/4)\exp(tR_2^2/4), \tag{3}$$

one can interpret the shrinkage of the diffractive cone as being due to an increase of the transverse spread of partons. In terms of the average parton momentum fraction, x, this implies that the transverse area occupied by the low virtuality partons in the hadron, R^2, increases with decreasing x roughly as [8]

$$R^2(x)=R_0^2+2\alpha'\ln(x_0/x). \tag{4}$$

Detailed information about the distribution of the *pp* cross section (both elastic and inelastic) over impact parameters can be obtained from the impact parameter representation of the *pp* elastic scattering amplitude; see, e.g., Ref. [2]. We write the invariant elastic amplitude in the form

$$A^{pp}(s,t)=\frac{is}{4\pi}\int d^2b e^{-i(\mathbf{\Delta}_\perp\mathbf{b})}\Gamma^{pp}(s,b) \tag{5}$$

$$=\frac{is}{2}\int_0^\infty dbbJ_0(\Delta_\perp b)\Gamma^{pp}(s,b), \tag{6}$$

where $\mathbf{\Delta}_\perp$ is a transverse momentum vector, with $t=-\mathbf{\Delta}_\perp^2$ and $\Delta_\perp\equiv|\mathbf{\Delta}_\perp|$, and J_0 denotes the Bessel function. Our normalization of the amplitude is the same as in Ref. [9], cf. the relation to the total cross section, Eq. (11) below. The dimensionless complex function Γ^{pp} is called the profile function of the elastic amplitude. In this representation the integrated cross section for elastic scattering is given by

$$\sigma_{\mathrm{el}}^{pp}(s)\equiv\frac{4\pi}{s^2}\int_{-s}^0 dt|A^{pp}(s,t)|^2 \tag{7}$$

$$=\int d^2b|\Gamma^{pp}(s,b)|^2. \tag{8}$$

In the last step, we have used that at large s the lower limit of the t integral can be replaced by $-\infty$, and that for an amplitude independent of the azimuthal scattering angle

$$\int_{-\infty}^0 dt=4\pi\int\frac{d^2\Delta_\perp}{(2\pi)^2}. \tag{9}$$

A similar representation can be derived for the total cross section for *pp* scattering, which by the optical theorem is proportional to the imaginary part of the forward ($t=0$) elastic amplitude:

$$\sigma_{\mathrm{tot}}^{pp}(s)=\frac{8\pi}{s}\mathrm{Im}\,A^{pp}(s,t=0) \tag{10}$$

$$=2\int d^2b\,\mathrm{Re}\,\Gamma^{pp}(s,b). \tag{11}$$

Finally, taking the difference of Eqs. (11) and (8), one obtains a representation of the inelastic (total minus elastic) *pp* cross section as an integral over impact parameters:

$$\sigma_{\mathrm{in}}^{pp}(s)\equiv\sigma_{\mathrm{tot}}^{pp}(s)-\sigma_{\mathrm{el}}^{pp}(s)$$

$$=\int d^2b[2\,\mathrm{Re}\,\Gamma^{pp}(s,b)-|\Gamma^{pp}(s,b)|^2]. \tag{12}$$

The integrand of Eq. (12) represents the distribution of the cross section for generic inelastic collisions (i.e., summed over all inelastic final states) over impact parameters. It is convenient to define a normalized b distribution as

$$P_{\mathrm{in}}(s,b)=\frac{2\,\mathrm{Re}\,\Gamma^{pp}(s,b)-|\Gamma^{pp}(s,b)|^2}{\sigma_{\mathrm{in}}(s)}. \tag{13}$$

For a quantitative estimate of this distribution we can use phenomenological parametrizations of the *pp* elastic scattering amplitude, which fit the presently available *pp* elastic data at collider energies. The results obtained with the parametrization of Islam *et al.* [9] (''diffractive'' part only) are presented in Fig. 3, for energies corresponding to RHIC and the LHC. It should be noted that the predictions for LHC are based on extrapolation of fits to the presently available data over nearly two orders of magnitude in s. The biggest uncertainty in the extrapolation appears to be due to the uncertainties in the measurement of $\sigma_{\mathrm{tot}}^{pp}$ at the Tevatron and the limited range of t covered in the collider measurements of elastic $\bar{p}p$ scattering.

In principle one should include here also effects of inelastic diffraction. However, this contribution should be rather small at LHC energies due to the blackening of interaction; see Ref. [10] for a recent review. Besides this, one expects that a significant part of inelastic diffraction at $t<0$ is due to the spin flip amplitudes [11].

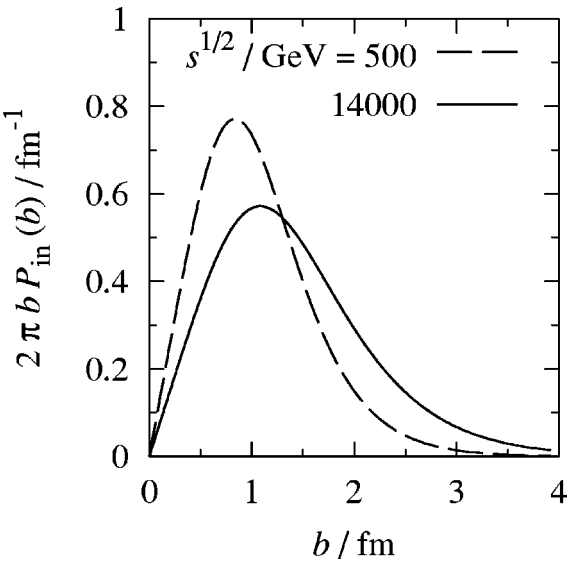

FIG. 3. The normalized impact parameter distribution for generic inelastic collisions, $P_{\rm in}(s,b)$, Eq. (13), obtained with the parametrization of the elastic *pp* amplitude of Islam *et al.* [9] ("diffractive" part only). The plot shows the "radial" distribution in the impact parameter plane, $2\pi b\, P_{\rm in}(s,b)$. The energies are $\sqrt{s}$ = 500 GeV (RHIC) and 14000 GeV (LHC).

III. TRANSVERSE SPATIAL DISTRIBUTION OF HARD PARTONS IN THE NUCLEON

We shall now review what is known about the transverse distribution of hard partons in the nucleon. Based on this, we shall later proceed to estimate the impact parameter distribution in *pp* collisions with hard dijet production.

Numerous measurements of hard inclusive scattering processes (DIS, Drell-Yan pair production) have produced a rather detailed picture of the longitudinal momentum distribution of partons in the nucleon. The study of the transverse spatial distribution of partons is still at a much more primitive stage. Information about the transverse spatial distribution of gluons is contained in the so-called two-gluon form factor of the nucleon, which parametrizes the t dependence of the (generalized) gluon distribution in the nucleon,

$$g(x,t;Q^2)=g(x;Q^2)F_g(x,t;Q^2), \tag{14}$$

where

$$F_g(x,t=0;Q^2)=1, \tag{15}$$

and $g(x;Q^2)$ is the usual gluon distribution in the nucleon. We define the Fourier transform of this form factor as

$$F_g(x,\rho;Q^2)\equiv\int \frac{d^2\Delta_\perp}{(2\pi)^2}e^{i(\boldsymbol{\Delta}_\perp\boldsymbol{\rho})}F_g(x,t=-\boldsymbol{\Delta}_\perp^2;Q^2), \tag{16}$$

where $\boldsymbol{\rho}$ is a two-dimensional coordinate variable, and $\rho\equiv|\boldsymbol{\rho}|$ (this variable is named $\boldsymbol{b}$ in Ref. [12]; in this paper we reserve $\boldsymbol{b}$ for the impact parameter vector of the *pp* collision). This function describes the spatial distribution of gluons in the transverse plane. It is normalized to unit integral over the transverse plane,

$$\int d^2\rho F_g(x,\rho;Q^2)=1. \tag{17}$$

A measure of the transverse size of the nucleon for given x and Q^2 is the average of ρ^2 calculated with this distribution, which is identical to 4 times the t slope of the two-gluon form factor at $t=0$,

$$\langle\rho^2\rangle(x,Q^2)\equiv\int d^2\rho\rho^2F_g(x,\rho;Q^2) \tag{18}$$

$$=4\frac{\partial}{\partial t}F_g(x,t;Q^2)|_{t=0}. \tag{19}$$

For sufficiently small $x(\lesssim 0.3)$ the parameter ρ can be interpreted as the distance of the parton from the center of mass of the nucleon in the transverse plane. For larger x the interpretation of the ρ distribution becomes less intuitive, as in this case one can no longer neglect the difference between the longitudinal momentum of the spectator system and that of the whole nucleon. In the limit $x\to 1$ the active parton would carry the entire longitudinal momentum of the nucleon, and only soft partons would be left in the spectator system; see Ref. [13] for a discussion. This shall not concern us here, since we shall be interested in the gluon distribution at $x\leqslant 0.05$, as relevant for hard dijet production in the central rapidity region (see below).

At moderately small $x(\gtrsim 0.001)$, it is possible to obtain information about the two-gluon form factor at a resolution scale of $Q_0^2\sim 2$–4 GeV^2 from the analysis of exclusive J/ψ photo (or electro) production off the nucleon [3]. It turns out that for $x\gtrsim 0.1$ this form factor is significantly harder than the electromagnetic form factor of the nucleon. The t dependence of the cross section is well described by a dipole form factor [3]

$$F_g(x,t)=\frac{1}{(1-t/m_g^2)^2}, \tag{20}$$

with a mass parameter

$$m_g^2\approx 1.1\ \text{GeV}^2\gg m_\rho^2 \quad (x\gtrsim 0.1). \tag{21}$$

The corresponding spatial distribution of gluons in the transverse plane, Eq. (16), is given by

$$F_g(x,\rho)=\frac{m_g^2}{2\pi}\left(\frac{m_g\rho}{2}\right)K_1(m_g\rho), \tag{22}$$

where K_1 denotes the modified Bessel function. Note that this function is positive, in agreement with the general positivity condition for the transverse coordinate-dependent gluon density, derived in Ref. [14]. The average $\langle\rho^2\rangle$ corresponding to this distribution is inversely proportional to the mass parameter squared,

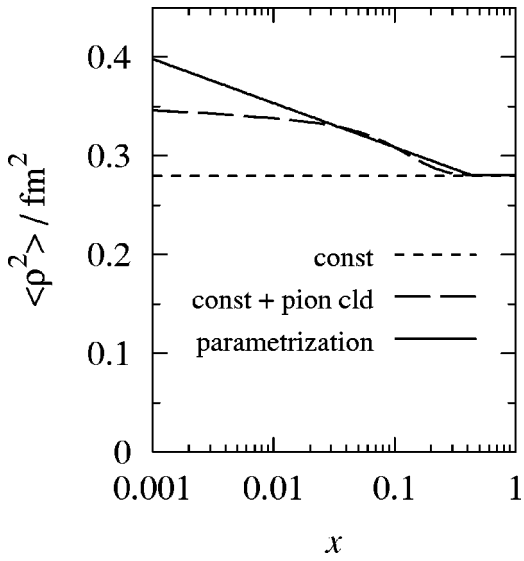

FIG. 4. Our model for the x dependence of the average transverse gluonic size squared of the nucleon, $\langle\rho^2\rangle$ at the scale $Q_0^2 = 2$–4 GeV^2 relevant to J/ψ production. *Short-dashed line*: $\langle\rho^2\rangle = 0.28$ fm^2, as extracted from the t-slope of the J/ψ production cross section measured in various experiments [3]. *Long-dashed line:* Sum of the constant value $\langle\rho^2\rangle = 0.28$ fm^2 and the pion cloud contribution calculated in Ref. [12]. *Solid line:* The parametrization Eq. (26), based on the experimental value of $\alpha'_{\rm hard}$, Eq. (25) [15].

$$\langle\rho^2\rangle = \frac{8}{m_g^2}. \tag{23}$$

Numerically, the value (21) amounts to

$$\langle\rho^2\rangle \approx 0.28 \ \text{fm}^2 \quad (x \gtrsim 0.1), \tag{24}$$

which is a factor of ~ 1.5 smaller than the proton's "transverse electric charge radius squared," $(2/3)\langle r^2\rangle_{\rm em}$.

For smaller values of $x (0.01 \lesssim x \lesssim 0.1)$ the transverse gluonic size of the nucleon starts to increase. This can be explained semiquantitatively by the kicking in of contributions from the pion cloud of the nucleon, which are suppressed for $x > M_\pi / M_N$ [12], see Fig. 4. The analysis of J/ψ photoproduction data has shown that the size keeps growing also for $x \lesssim 0.01$ [15]. In all, the rate of the increase of the gluonic size between $x \sim 10^{-2}$ and 10^{-3} is about a factor of two *smaller* than that of the total cross section, which is dominated by soft physics (see Sec. II):

$$\frac{1}{4}\frac{\partial\langle\rho^2\rangle}{\partial \ln(1/x)} \equiv \alpha'_{\rm hard} \approx 0.125 \ \text{GeV}^{-2}$$

$$(x = 10^{-3}\text{–}10^{-2}), \tag{25}$$

which should be compared with Eq. (2). We can parametrize the x dependence of $\langle\rho^2\rangle$, at the scale Q_0^2 probed in J/ψ production, by combining this experimentally determined rate of increase with our model estimate of $\langle\rho^2\rangle$ (constant plus pion cloud contribution) at $x = 0.1$, $\langle\rho^2\rangle = 0.31$ fm^2 [12]. This amounts to the parametrization

$$\langle\rho^2\rangle(x, Q_0^2) = \max\left\{ \begin{array}{l} 0.31 \ \text{fm}^2 + 0.0194 \ \text{fm}^2 \ \ln\dfrac{0.1}{x}, \\ 0.28 \ \text{fm}^2. \end{array} \right. \tag{26}$$

This simple form fits well the x dependence of $\langle\rho^2\rangle$ due to pion cloud contributions in the region $0.01 \leqslant x \leqslant 0.1$, as calculated in Ref. [12], see Fig. 4, and continues it down to smaller values of x using the experimentally measured rate of increase.

For our estimates of the probability of hard multijet production we need to model not only the average transverse size of the nucleon, but the full transverse spatial distribution of gluons. For simplicity, we shall assume that at the scale Q_0^2 the ρ distribution at all relevant x can be described by the Fourier transform of a dipole form factor, cf. Eq. (22), but with an x-dependent mass parameter. This parameter is then uniquely determined by the value of $\langle\rho^2\rangle$, as given by Eq. (26), via Eq. (23). This defines our model of the x- and ρ-dependent distribution of gluons at the scale Q_0^2.

We are interested in the ρ-dependent gluon distribution at large virtualities, corresponding to hard dijet production at LHC. This requires to take into account the effect of DGLAP evolution on the ρ-dependent distributions. The Q^2 evolution of the parton distributions is diagonal in ρ. It degrades the longitudinal momentum fractions x of the partons, resolving a parton with given x into a collection of partons with smaller x, while the transverse location of the new partons is practically the same as that of the "parent" parton provided $Q \gg 1/\rho$. Nevertheless, Q^2 evolution does change the ρ profile of the distributions at given x. Generally speaking, evolution will reduce the rate of broadening of the distributions with decreasing of x. This happens because with increasing Q^2 the parton distributions at the high scale become sensitive to the input distribution at the low scale Q_0^2 at larger and larger x values, where their transverse size becomes small.

We have studied numerically the leading-order Q^2 evolution of our model of the ρ-dependent gluon distribution at the scale Q_0^2 cf. Eqs. (22), (26) and (23), employing the numerical method described in Ref. [16]. We have used the Glück-Reya-Vogt leading-order parametrization [17] to describe the total (integrated over ρ) gluon and singlet quark distributions at the input scale Q_0^2 and modeled their ρ profile as described above. The value of the input scale we have taken as $Q_0^2 = 3$ GeV^2, which is the central value of the range of scales associated with J/ψ photoproduction. For simplicity we assume identical ρ profiles for the gluon and singlet quark distributions at the input scale. The results of the DGLAP evolution of the ρ-dependent gluon distribution are shown in Figs. 5 and 6. Figure 5 shows the normalized ρ profile, $F_g(x, \rho; Q^2)$, cf. Eq. (16), corresponding to the distribution after evolving to the higher scale Q^2, for the value $x = 10^{-3}$. Figure 6 shows the Q^2 dependence of the average size squared, $\langle\rho^2\rangle$, as induced by DGLAP evolution, for values of $x = 10^{-2}, 10^{-3}$ and 10^{-4}. The corresponding curves for the singlet quark distribution would be qualitatively similar. One can see that the effect of transverse broadening of the gluon distribution with decreasing x, which is rather

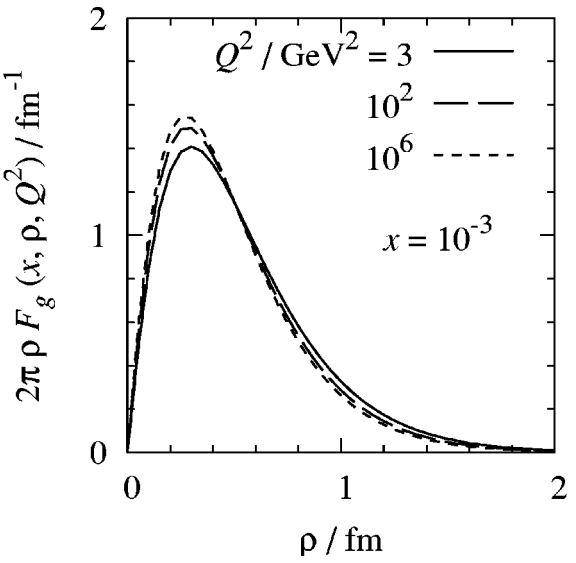

FIG. 5. The change of the normalized ρ profile of the gluon distribution, $F_g(x,\rho;Q^2)$, Eq. (16), with Q^2, as due to DGLAP evolution, for $x=10^{-3}$. The input gluon distribution is the Glück-Reya-Vogt parametrization at $Q_0^2=3$ GeV^2, with a dipole-type ρ profile, Eq. (22), of size determined by the parametrization Eq. (26).

small already at the initial resolution scale, is further reduced at the scale relevant for the LHC kinematics ($Q \geqslant 20$ GeV).

Figure 5 demonstrates that the deviations of the ρ profile from the dipole shape at the initial scale, Eqs. (22), due to DGLAP evolution are very small. This suggests a simplified parametrization of the combined Q^2 and x dependence of the ρ profile of the gluon distribution, in which the dipole shape is assumed to hold at all Q^2 (and x), and the Q^2 (and x) dependence is entirely ascribed to the mass parameter m_g^2. We fit the combined Q^2 and x dependence of $\langle\rho^2\rangle$ due to

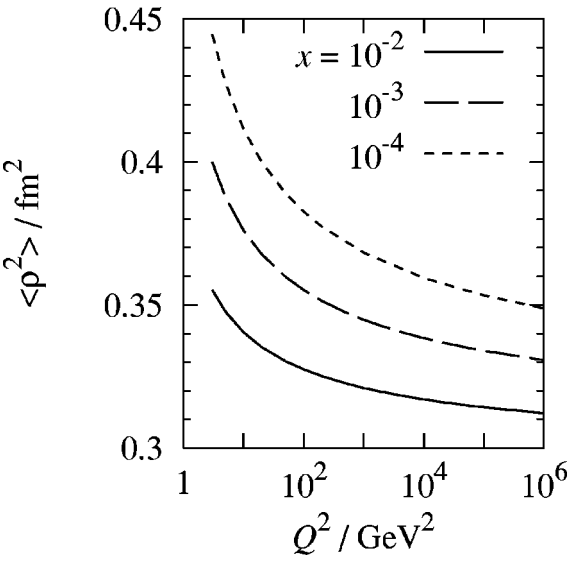

FIG. 6. The change of the average transverse gluonic size squared, $\langle\rho^2\rangle$, due to DGLAP evolution, for $x=10^{-2}, 10^{-3}$ and 10^{-4}.

DGLAP evolution in the region $Q_0^2 \leqslant Q^2 \leqslant 10^6$ GeV^2, as shown in Fig. 6, by the simple two-parameter form

$$\langle\rho^2\rangle(x,Q^2)=\langle\rho^2\rangle(x,Q_0^2)\left(1+A\ln\frac{Q^2}{Q_0^2}\right)^{-a}, \qquad (27)$$

where $Q_0^2=3$ GeV^2, $\langle\rho^2\rangle(x,Q_0^2)$ is defined by Eq. (26), and

$$A=1.5, \quad a=0.0090\ln\frac{1}{x}. \qquad (28)$$

For each x and Q^2, this value of $\langle\rho^2\rangle$ defines a dipole mass parameter m_g^2 via Eq. (23). Our model for the ρ-dependent gluon distribution is then given by the Glück-Reya-Vogt leading-order parametrization for the total distribution at the scale Q^2, times the normalized dipole ρ profile, Eq. (22), with this mass parameter. This parametrization has the correct Q^2 dependence of the transverse size is ''built in,'' removing the need to perform explicit DGLAP evolution of the ρ-dependent distributions, which is very convenient for the following studies.

IV. IMPACT PARAMETER DISTRIBUTION FOR A HARD MULTIJET TRIGGER

Using the information about the transverse distribution of partons in the proton, we can now investigate the impact parameter dependence of the cross section for inelastic collisions with production of two jets in the central rapidity region. In particular, we shall show that a trigger on hard dijet events allows to reduce the effective impact parameters of pp collisions as compared to generic inelastic collisions studied in Sec. II.

We consider the production of two jets (with equal but opposite transverse momentum) in a binary parton-parton collision. The resolution scale is given by the transverse momentum squared of one of the jets, $q_\perp^2$. The momentum fractions of the two colliding partons with respect to their parent protons, x_1 and x_2, can be reconstructed from the measured energy and momenta of the two jets. Four-momentum conservation implies for the scattering at 90° at the center of mass of two partons

$$x_1x_2=\frac{4q_\perp^2}{s}, \qquad (29)$$

where $4q_\perp^2$ is the invariant mass squared of the two-jet system. In the following we shall be interested in two jets near zero total rapidity, which requires

$$x_1\approx x_2. \qquad (30)$$

Under this condition the momentum fractions are completely fixed by Eq. (29). In the following we consider the dijet production due to collision of two gluons, since such partonic collisions give the dominant contribution to the total cross section. The probability for a binary collision of two gluons is proportional to the product of the gluon densities in transverse space in the two colliding protons, taking into

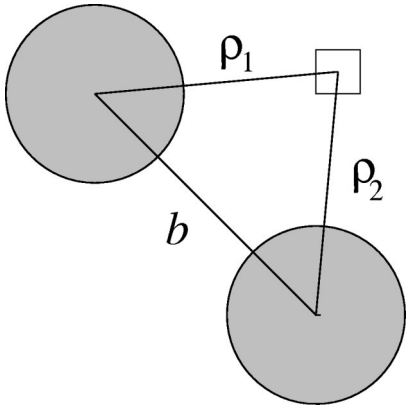

FIG. 7. Illustration of the overlap integral of parton distributions in the transverse plane, defining the b distribution for binary parton collisions producing a dijet, Eq. (31).

account that their transverse centers are separated by a distance b—the impact parameter of the pp collision; see Fig. 7. This implies that the distribution of the cross section for such events over the impact parameter b is given by

$$P_2(b) \equiv \int d^2\rho_1 \int d^2\rho_2 \delta^{(2)}(\boldsymbol{b}-\boldsymbol{\rho}_1+\boldsymbol{\rho}_2) \times F_g(x_1,\rho_1)F_g(x_1,\rho_2), \tag{31}$$

where $x_1 = 2q_\perp/\sqrt{s}$, cf. Eqs. (29) and (30), and the scale of the gluon ρ profiles is $q_\perp^2$. This distribution is normalized such that the integral over all $\boldsymbol{b}$ is unity. Since it has the form of a convolution in the parton transverse positions, it can also be expressed as the Fourier transform of the square of the two-gluon form factor, Eq. (20). In particular, for the two-gluon form factor of dipole form, Eq. (22), used in our model of the ρ-dependent gluon distribution (see Sec. III) one obtains

$$P_2(b) = \frac{m_g^2}{12\pi}\left(\frac{m_g b}{2}\right)^3 K_3(m_g b), \tag{32}$$

where m_g should be substituted by the value corresponding to $x_1 = 2q_\perp/\sqrt{s}$ and $Q^2 = q_\perp^2$, see Eq. (27).

Figure 8 shows the distribution $P_2(b)$ for a center-of-mass energy of $\sqrt{s} = 14000$ GeV (LHC), and two values of the jet momentum, $q_\perp = 10$ GeV and 100 GeV. One sees that the distribution is rather insensitive to the precise value of the jet momentum. This can be explained by the relatively slow decrease of $\langle \rho^2 \rangle$ with increasing x and Q^2. The average values of impact parameter squared, $\langle b^2 \rangle$, calculated with these distributions, is 0.71 fm^2 for $q_\perp = 10$ GeV and 0.63 fm^2 for $q_\perp = 100$ GeV.

In Fig. 8 we assume production of a two-jet system at zero rapidity, cf. Eq. (30). If we considered instead a two-jet system at some nonzero rapidity, y, the (anyway weak) dependence of the ρ distributions in Eq. (31) on x_1 and x_2 would work in opposite directions, leading to an extremely weak dependence of our results on the rapidity of the produced system over a wide range of y.

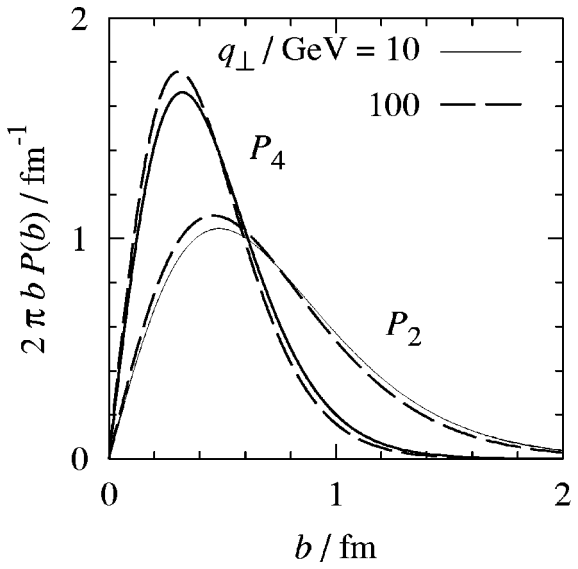

FIG. 8. The b distribution for the trigger on hard dijet production, $P_2(b)$, obtained with the dipole form of the gluon b profile, Eq. (32), for $\sqrt{s} = 14000$ GeV and $q_\perp = 10$ GeV and 100 GeV. The plots show the "radial" distributions in the impact parameter plane, $2\pi b P_2(b)$. Also shown is the corresponding distribution for a trigger on double dijet production, $P_4(b)$, with the same $p_\perp$.

In Fig. 9 we compare the b distribution for the hard dijet trigger, $P_2(b)$ (solid line), with the b distribution for generic inelastic events, $P_{\rm in}(s)$, estimated in Sec. II. The short-dashed line in Fig. 9 shows the distribution $P_{\rm in}(s)$ obtained from the parametrization of the elastic pp amplitude of Islam *et al.* [9] ("diffractive" part only). Shown are the results for $\sqrt{s} = 14000$ GeV (LHC), 1800 GeV (Tevatron $\overline{p}p$), and 500 GeV (RHIC). A momentum of $q_\perp = 25$ GeV was assumed for the dijet trigger. One sees that in all cases the b distribution for dijet events is much narrower than the one for generic inelastic collisions. The corresponding averages $\langle b^2 \rangle$ are given in Table I. The average $\langle b^2 \rangle$ for the hard dijet trigger rises much more slowly with s than for generic inelastic collisions, which are dominated by soft physics. Thus, the reduction in effective impact parameters due to the dijet trigger is most pronounced at LHC energies, where $\langle b^2 \rangle$ is reduced to $\sim 1/4$ its value for generic inelastic collisions.

A further reduction of the effective impact parameters can be achieved by a trigger on events with two dijets, i.e., two binary hard parton collisions (such processes can be easily distinguished from the leading twist $2 \to 4$ processes in the collider experiments; see, e.g., Ref. [7]). It was estimated in Ref. [18] that this reduces $\langle b^2 \rangle$ by a factor of two as compared to the single dijet trigger. In our approach, the b distribution for the double dijet trigger is given by

$$P_4(b) = \frac{P_2^2(b)}{\int d^2b P_2^2(b)}. \tag{33}$$

For simplicity we assume here identical x_1 and $q_\perp$ for the

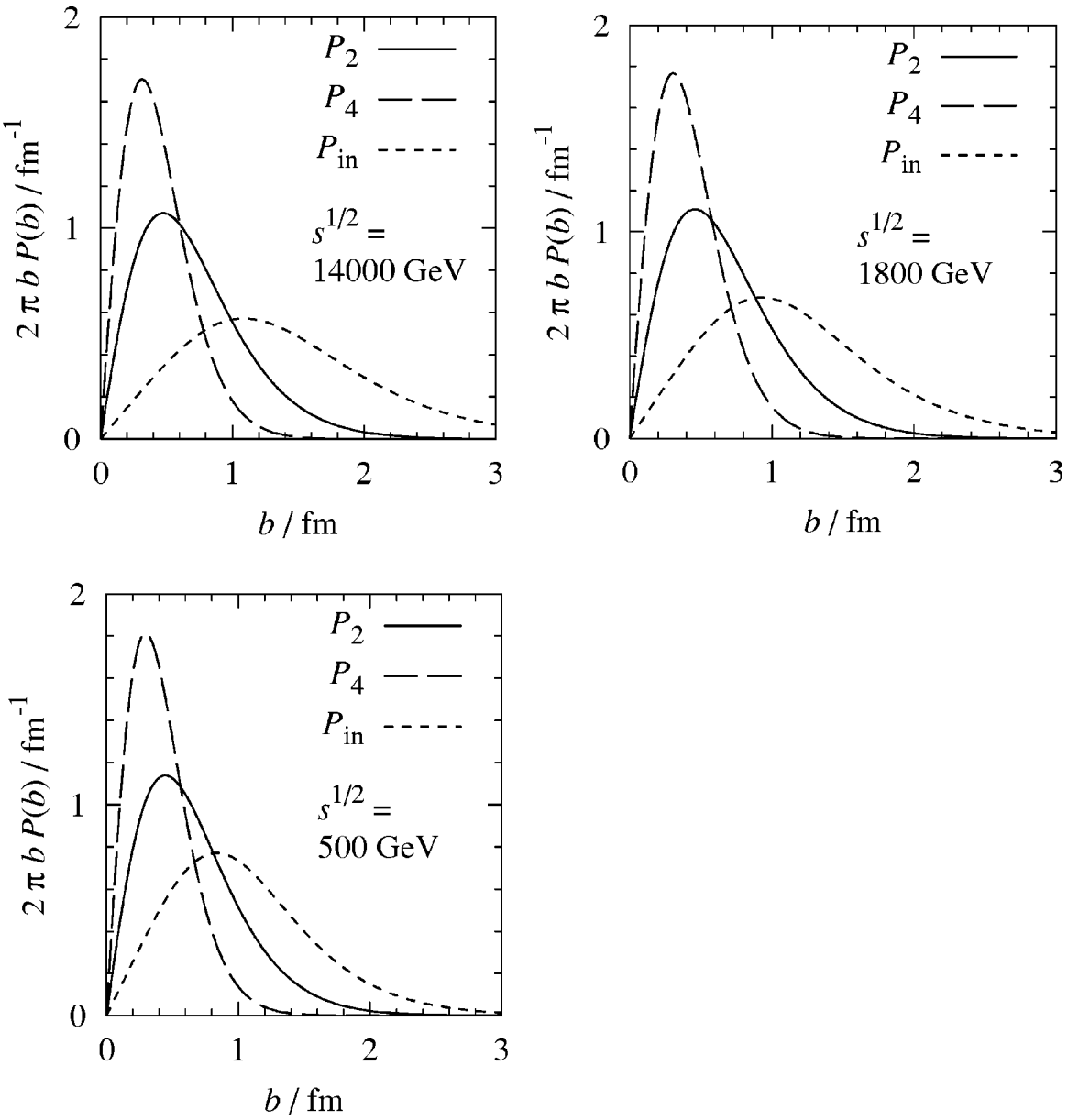

FIG. 9. *Solid lines: b* distributions for the dijet trigger, $P_2(b)$, with $q_\perp = 25$ GeV, as obtained from the dipole-type gluon ρ profile, Eq. (32). *Long-dashed line: b* distribution for double dijet events, $P_4(b)$. *Short-dashed line*: *b* distribution for generic inelastic collisions, obtained from the parametrization of the elastic *pp* amplitude of Islam *et al.* [9] (''diffractive'' part only), cf. Fig. 3. Shown are the results for $\sqrt{s} = 14000$ GeV (LHC), 1800 GeV (Tevatron $\bar{p}p$), and 500 GeV (RHIC). The plots show the ''radial'' distributions in the impact parameter plane, $2\pi b P(b)$.

two dijets; the definition could easily be generalized to allow for different values. For the two-gluon form factor of dipole form, Eq. (22), this becomes

$$P_4(b) = \frac{7m_g^2}{36\pi}\left(\frac{m_g b}{2}\right)^6 [K_3(m_g b)]^2, \tag{34}$$

where again m_g should be substituted by the value corresponding to $x_1 = 2q_\perp/\sqrt{s}$ and $Q^2 = q_\perp^2$, see Eq. (27). Figure 8 shows that the *b* distribution for the double dijet trigger, $P_4(b)$, is equally insensitive to the precise value of $q_\perp$ as that for the dijet trigger, $P_2(b)$. The comparison in Fig. 9 and Table I shows that the double dijet trigger allows for a further reduction of the effective impact parameters by a factor of ~ 2.5 compared to the dijet trigger.

In calculating $P_4(b)$ we have made the assumption that the gluons are not correlated in the transverse plane. To test this assumption we can compare the rate of double dijet production in our model to the one which is observed in the CDF experiment [7]. The ratio of the cross section of double dijet events and the square of the single dijet cross section is proportional to [7,19]

TABLE I. The average impact parameter squared, $\langle b^2\rangle$, corresponding to the b distributions $P_2(b)$,$P_4(b)$, and $P_{\rm in}(b)$, shown in Fig. 9.

Facility	$\sqrt{s}$/GeV	$\langle b^2\rangle_2$/fm^2	$\langle b^2\rangle_4$/fm^2	$\langle b^2\rangle_{\rm in}$/fm^2
LHC	14000	0.67	0.26	2.7
Tevatron	1800	0.63	0.24	1.8
RHIC	500	0.59	0.23	1.43

$$\sigma_{\rm eff}=\left[\int d^2b P_2^2(b)\right]^{-1}. \tag{35}$$

In our calculation we find $\sigma_{\rm eff}=34$ mb, which should be compared with $\sigma_{\rm eff}=14.5\pm1.7^{+1.7}_{-2.3}$ mb reported by CDF assuming that there is no correlations in the longitudinal distribution of partons. (In Ref. [19] $\sigma_{\rm eff}\sim30$ mb was obtained assuming that the parton distribution is similar to that of valence quarks, a hypothesis resembling the conclusion we derived from the leading twist analysis of the J/ψ elastic photoproduction [3].) A factor of two difference between the theoretical number and the data may indicate that there are significant transverse correlations in the parton density at the resolution scale of $Q\geqslant5$ GeV probed by CDF. Such correlations could result, for example, due to the DGLAP evolution from a low Q^2 scale of a couple GeV^2 to $Q\sim25$ GeV^2, since the partons emitted in the course of this evolution would have small transverse separation (the so-called ''hot spots'' of Ref. [20]). Assuming that the difference between the uncorrelated model and the data is due to such *local correlations in b* we would obtain a b distribution for the double dijet trigger approximately as

$$P_{4,\rm corr}(b)\approx P_2(b)\frac{\sigma_{\rm eff}(\rm model)-\sigma_{\rm eff}(\rm CDF)}{\sigma_{\rm eff}(\rm model)}+P_4(b)\frac{\sigma_{\rm eff}(\rm CDF)}{\sigma_{\rm eff}(\rm model)}, \tag{36}$$

where $P_2(b)$ and $P_4(b)$ are the above uncorrelated model estimates. It is clear from the inspection of Fig. 9 that this still corresponds to a large reduction (by a factor ~1.5) of the effective impact parameters with the double dijet trigger as compared to the single dijet trigger.

It should be noted that the jet cross sections discussed here are sensitive to the choice of ''primordial'' transverse momentum distribution of the colliding partons, to higher-order radiative corrections, and to the jet definition adopted. To our knowledge, the same procedure was used in analyzing single and double dijet events in Ref. [7] (one of the jets was taken to be a photon for simplicity), so most of these effects should cancel in the cross section ratio. An additional source of uncertainty is the correlation of the soft background in hadron production with the centrality of the pp event, as discussed in Sec. VI. A quantitative study of parton-parton correlations certainly requires a more careful investigation of these effects.

To summarize, we have demonstrated that a trigger on events with (one or more) dijets near zero rapidity strongly reduces the effective impact parameters in pp collisions at LHC energies. Such a trigger can thus be used as a ''centrality filter.'' This is of considerable practical interest, as the characteristics of the final state strongly depend on the centrality of the pp collision.

V. APPROACHING THE BLACKBODY LIMIT IN CENTRAL pp COLLISIONS

An interesting feature of central pp collisions at high energies is that large-x partons ($x\geqslant0.01$) in one nucleon pass through a strong gluon field in the other nucleon. This field can become so strong that the interaction of the parton with the other nucleon approaches the blackbody limit (BBL), in which the probability for inelastic scattering becomes unity, and the cross section becomes comparable to the transverse size of the strong gluon field. This phenomenon would have dramatic consequences for particle production in the forward region (dilepton production, hadron multiplicities and transverse momentum distributions), which have become the subject of intensive theoretical investigation. In this section we want to quantify the proximity to the BBL for pp collisions at LHC energies. Specifically, we want to show how a trigger on hard dijet (or multijet) production, which reduces the effective impact parameters in pp collisions, greatly increases the region (in the momentum fraction, x, and the virtuality, Q^2) in which partons experience interactions close to the BBL. For a recent review of approaches to ''taming'' the growth of parton densities at small x, based on the impact parameter eikonal approximation and the leading-log$x$ approximation, see Refs. [21].

To simplify the discussion, we consider instead of the scattering of a colored parton the scattering of a small color-singlet dipole off the other nucleon. This is in the spirit of the dipole picture of high-energy scattering of Mueller [22]. The distribution of the inelastic and elastic cross sections, $\sigma_{\rm in}^{dp}$ and $\sigma_{\rm el}^{dp}$, over the dipole-proton impact parameter, ρ, can be expressed in terms of the profile function of the dipole-nucleon elastic scattering amplitude, $\Gamma^{dp}(s,\rho)$ (cf. Sec. II):

$$\sigma_{\rm in,el}^{dp}(s)=\int d^2\rho\,\sigma_{\rm in,el}^{dp}(s,\rho), \tag{37}$$

with

$$\sigma_{\rm el}^{dp}(s,\rho)=|\Gamma^{dp}(s,\rho)|^2, \tag{38}$$

$$\sigma_{\rm in}^{dp}(s,\rho)=2\,{\rm Re}\,\Gamma^{dp}(s,\rho)-|\Gamma^{dp}(s,\rho)|^2. \tag{39}$$

The functions $\sigma_{\rm in,el}^{dp}(s,\rho)$ are dimensionless and can be interpreted as the ''cross sections per unit transverse area.'' If the target proton were a ''black'' disk of radius R, the probability for a dipole hitting the target to undergo inelastic scattering would be unity, and one would have $\sigma_{\rm in}^{dp}(s,\rho)=1$ for $\rho<R$. This would imply

$$\Gamma^{dp}(s,\rho)=1 \quad \text{for } \rho<R. \tag{40}$$

From Eq. (38) it follows that in this case the elastic cross section would also be unity,

$$\sigma_{\rm el}^{dp}(s,\rho)=1 \quad \text{for} \quad \rho<R, \tag{41}$$

and thus the total (elastic plus inelastic) cross section would be twice the inelastic one. For realistic interactions, one may say that the proton becomes black if $\Gamma^{dp}(s,\rho)$ approaches unity in a certain region of impact parameters. In the following we shall use this criterion to quantify the approach of dipole-nucleon interactions to the BBL. A similar approach was used in Ref. [23] to study the proximity of $\gamma^* N$ scattering to the BBL.

For small dipole sizes the cross section for inelastic dipole-nucleon scattering at fixed impact parameter b is given by the leading-twist perturbative QCD expression [24,25]

$$\sigma_{\rm in,LT}^{dp}(s,\rho)=\frac{C\pi^2}{3}d^2\alpha_s(Q^2)x' g(x',\rho;Q^2). \tag{42}$$

Here C is a color factor,

$$C=\begin{cases}1, & 3\bar{3} \text{ dipole},\\ 9/4, & 88 \text{ dipole},\end{cases} \tag{43}$$

d is the dipole size, $\alpha_s(Q^2)$ the leading-order QCD running coupling,

$$\alpha_s(Q^2)=\frac{4\pi}{\beta_0 \ln(Q^2/\Lambda^2_{\rm QCD})}, \tag{44}$$

$$\beta_0\equiv\frac{11}{3}N_c-\frac{2}{3}N_f \tag{45}$$

($\Lambda_{\rm QCD}$ is the scale parameter), and $g(x,\rho;Q^2)$ the impact parameter-dependent leading twist gluon density in the nucleon,

$$g(x',\rho;Q^2)\equiv g(x',Q^2)F_g(x',\rho;Q^2), \tag{46}$$

where $g(x',Q^2)$ is the usual (total) gluon density and $F_g(x',\rho;Q^2)$ the normalized ρ profile, Eq. (16). The scale parameter Q^2 in α_s and the gluon density is related to the dipole size by

$$Q^2=\frac{\lambda}{d^2}, \tag{47}$$

where λ is a dimensionless parameter whose value is to be determined from phenomenological considerations. A value of $\lambda=9$ sets d equal to the average dipole size contributing to the longitudinal photon-nucleon cross section at large Q^2; we shall use this value of λ in the following. The gluon momentum fraction probed in inelastic dipole-nucleon scattering is determined by the invariant mass squared of the produced system, M^2,

$$x'=\frac{M^2+Q^2}{s}. \tag{48}$$

Here we have in mind generic inelastic production with $M^2\sim Q^2$, so we take

$$x'\approx\frac{2Q^2}{s}=2x \tag{49}$$

as the argument for the gluon distribution. In the following we shall regard the cross section viz. the profile function as a function of $x=Q^2/s$ and the dipole-proton impact parameter, ρ.

Comparing Eqs. (39) and (42) we obtain an equation for the profile function Γ (regarded now as a function of x and ρ) corresponding to the leading-twist QCD result. If we assume the elastic amplitude to be imaginary, i.e., Γ to be real, we obtain

$$2\Gamma^{dp}-(\Gamma^{dp})^2=\sigma_{\rm in,LT}^{dp}. \tag{50}$$

The relevant solution of this quadratic equation is

$$\Gamma^{dp}(x,\rho)=1-\sqrt{1-\sigma_{\rm in,LT}^{dp}(x,\rho)}. \tag{51}$$

Note that this solution implies that $\Gamma^{dp}\to 0$, and thus $\sigma_{\rm el}\to 0$ [cf. Eq. (38)], for $\sigma_{\rm in,LT}\to 0$, i.e., in the limit of small dipole size. For the corresponding solution with the "+" sign in front of the square root the elastic cross section would tend to a constant value for zero dipole size.

We evaluate the leading-twist expression for the inelastic 88 dipole-nucleon cross section (42) with the model for the ρ-dependent gluon distribution described in Sec. III based on the dipole form factor with x- and Q^2-dependent mass parameter. Figure 10 shows the profile function $\Gamma^{dp}(x,\rho)$ obtained from Eq. (51) for values $x=10^{-2}$, 10^{-3} and 10^{-4}, and $Q^2=100$, 50 and 20 GeV^2; the dipole size in each case is determined as $d^2=\lambda/Q^2$ with $\lambda=9$. The results clearly show the approach to the BBL for decreasing x (as a result of the growth of the gluon density) and/or decreasing Q^2 (as a result of the increasing dipole size). Note that the results for the profile function shown here are physically meaningful only in the region of impact parameters where Γ^{dp} is significantly less than unity; for $\Gamma^{dp}\sim 1$ the simple leading-twist formula for the inelastic dipole-nucleon cross section, Eq. (42), breaks down. In other words, the figures should be read as indicating the *region in impact parameter* for which the cross section approaches the BBL, rather than *how* it is approached once the interaction is sizable. An objective measure of the size of this region is the value of ρ at which Γ^{dp} exceeds a certain critical value, $\Gamma_{\rm crit}$,

$$\Gamma^{dp}(x,\rho)\geqslant\Gamma^{dp}_{\rm crit} \quad \text{for} \quad \rho<\rho_{\rm crit}. \tag{52}$$

Figure 11 shows $\rho_{\rm crit}$ as a function of x, and for the above values of Q^2, for $\Gamma^{dp}_{\rm crit}=0.5$. This value of Γ^{dp} corresponds to a probability of having no inelastic interaction of only 0.25, cf. Eq. (39), which is a reasonable guideline. In Fig. 11 a value of $\rho_{\rm crit}=0$ implies that $\Gamma^{dp}(x,\rho)$ is smaller than $\Gamma^{dp}_{\rm crit}$ for all values of ρ; even in the center of the nucleon where the gluon density is maximum ($\rho=0$).

We now turn to the question under which conditions in proton-proton collisions a parton in one proton will interact

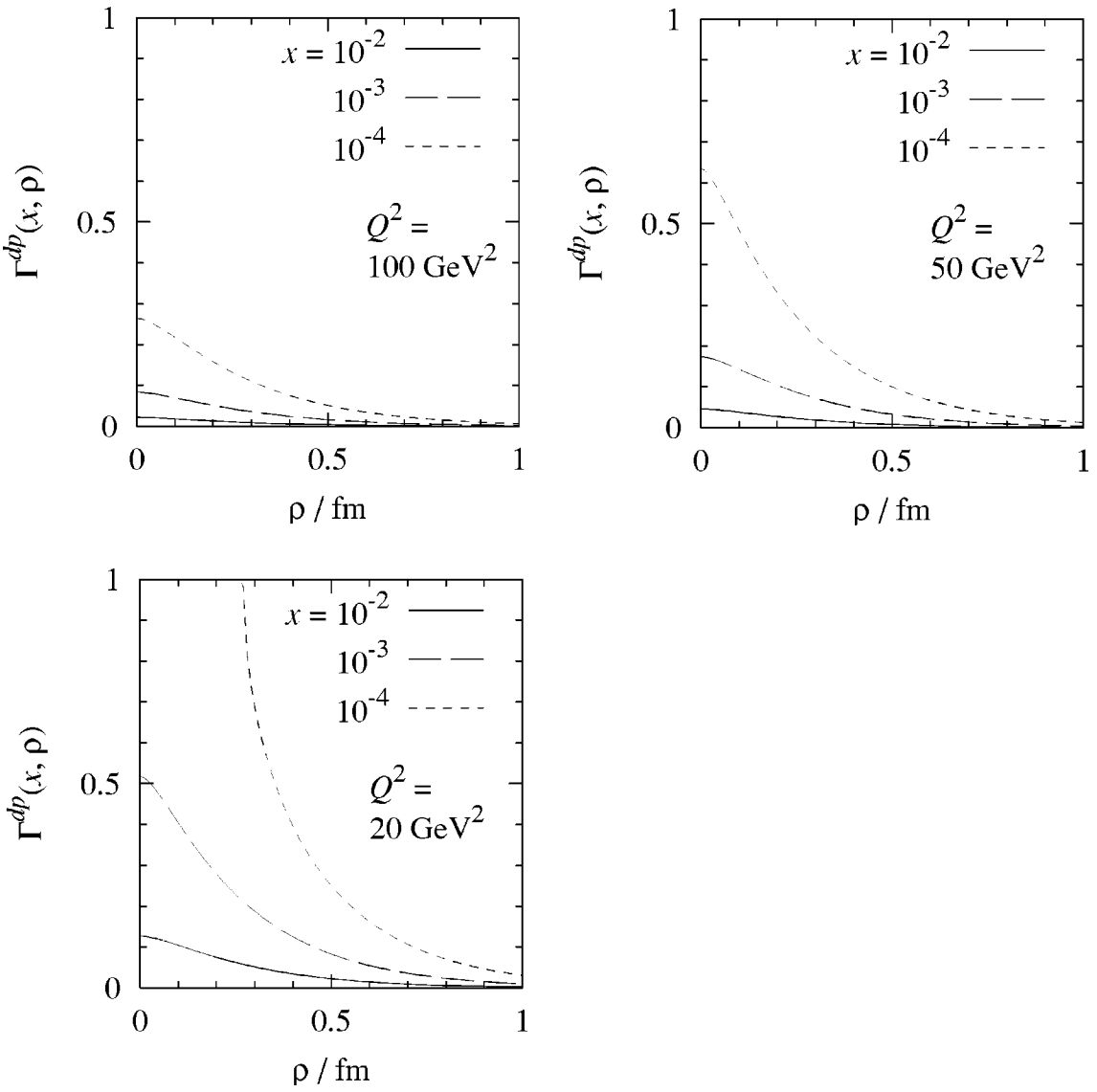

FIG. 10. The profile function for elastic dipole-nucleon scattering, $\Gamma^{dp}(x,\rho)$, obtained from Eq. (51) with the inelastic cross section given by the leading-twist expression, Eq. (42). Shown are the results for an 88 dipole with $Q^2=100$ GeV^2 (upper left panel), 50 GeV^2 (upper right panel), and 20 GeV^2 (lower left panel), for various values of x.

with the gluon field in the other proton near the BBL. The probability for this to happen depends on the transverse position of the parton relative to the center of its parent proton, ρ_1, as well as the impact parameter of the proton-proton collision. An interesting measure is the total probability for partons in one proton with given momentum fraction x and virtuality Q^2 (but arbitrary transverse position) to interact with the other proton near the BBL. It is given by the overlap integral of the normalized transverse spatial distribution of the partons in their parent proton (shifted by the impact parameter vector, $\boldsymbol{b}$), with the characteristic function of the ''black'' region in the other proton, $\Theta(\rho_1<\rho_{\rm crit})$,

$$P_{\rm black}(b)\equiv\int d^2\rho_1\Theta(\rho_1<\rho_{\rm crit})F_g(x,\rho_2)$$
$$(\rho_2\equiv|\boldsymbol{\rho}_1-\boldsymbol{b}|). \qquad (53)$$

This integral measures the fraction of the partons with given x and Q^2 which hit the other proton in the ''black'' central region. Here $\rho_{\rm crit}$ depends on x and Q^2, see above. Generally, the probability $P_{\rm black}(b)$ is maximum for central collisions ($b=0$) and decreases with increasing b. Note that if the target proton were a ''black'' disk of radius R, and the parent proton of the parton a disk of same size, $P_{\rm black}$ would be unity at $b=0$. Figure 12 shows $P_{\rm black}(b)$ for partons with virtuality $Q^2=20$ GeV^2 and different values of x.

In actual hadron-hadron collisions, the parton which probes the gluon field in the other proton is resolved by a hard collision with a parton in the other proton, resulting in hadron production; see Fig. 2. Let x_R be the momentum fraction of the resolving parton. Production of hadrons with transverse momentum $p_\perp$ then resolves partons with momentum fraction [cf. Eq. (1)]

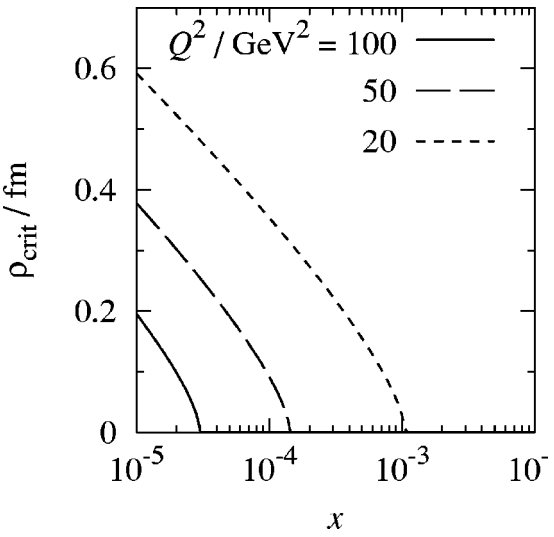

FIG. 11. The critical value of impact parameter, $\rho_{\rm crit}$, for which the profile function of elastic dipole-nucleon scattering, $\Gamma^{dp}(x,\rho)$, exceeds the value $\Gamma^{dp}_{\rm crit}=0.5$, cf. Eq. (52). Here $\rho_{\rm crit}$ is shown as a function of x. A value of $\rho_{\rm crit}=0$ implies that $\Gamma^{dp}(x,\rho)<\Gamma^{dp}_{\rm crit}$ for all values of ρ. Shown are the results for an 88 dipole; the Q^2 values are the same as in Fig. 10.

$$x=\frac{4p_\perp^2}{x_R s} \tag{54}$$

and virtuality

$$Q^2=4p_\perp^2\,. \tag{55}$$

We are interested in partons with relatively large x_R ($\sim 10^{-1}$), which are able to resolve small-x partons in the other proton whose interactions are close to the BBL. Generally speaking, large $p_\perp$ select partons with large x and large Q^2, for which interactions close to the BBL are unlikely. Thus, the probability of interactions close to the BBL decreases with increasing $p_\perp$. On the other hand, a certain minimum value of the parton virtuality, Q^2, and thus of $p_\perp$, is required for the concept of parton resolution by jet production to be applicable. Thus, it is crucial to establish that there is a "window" in $p_\perp$ in which one is sensitive to BBL effects while at the same time the partonic description is still applicable.

An important quantity is the maximum value of $p_\perp$ (for given x_R) for which the resolved parton sees the other proton as "black." We can estimate this maximum $p_\perp$ with the help of the probability $P_{\rm black}$ introduced in Eq. (53). For given x_R, and given impact parameter b, we ask for the maximum value of $p_\perp^2$ for which $P_{\rm black}(b)$ exceeds a certain critical value:

$$P_{\rm black}(b)>P_{\rm crit} \quad \text{for} \quad p_\perp^2<p_{\perp,\rm BBL}^2\,. \tag{56}$$

Figure 13 shows $p_{\perp,\rm BBL}^2$ corresponding to the criterion that $P_{\rm black}(b)>0.5$, as a function of the impact parameter of the proton-proton collision, b. One sees that the maximum $p_\perp$ drops rapidly with increasing b. [For $b\gtrsim 1$ fm the maximum value of $p_\perp^2$ defined according to Eq. (56) becomes <1 GeV^2 and thus physically meaningless.] For central collisions, $b<0.5$ fm, the values of $p_{\perp,\rm BBL}^2$ are larger than 10 GeV^2, so that the underlying leading-twist approximation is well justified. For such impact parameters it is possible to explore the properties of the BBL using resolved hard partons as a well-defined probe.

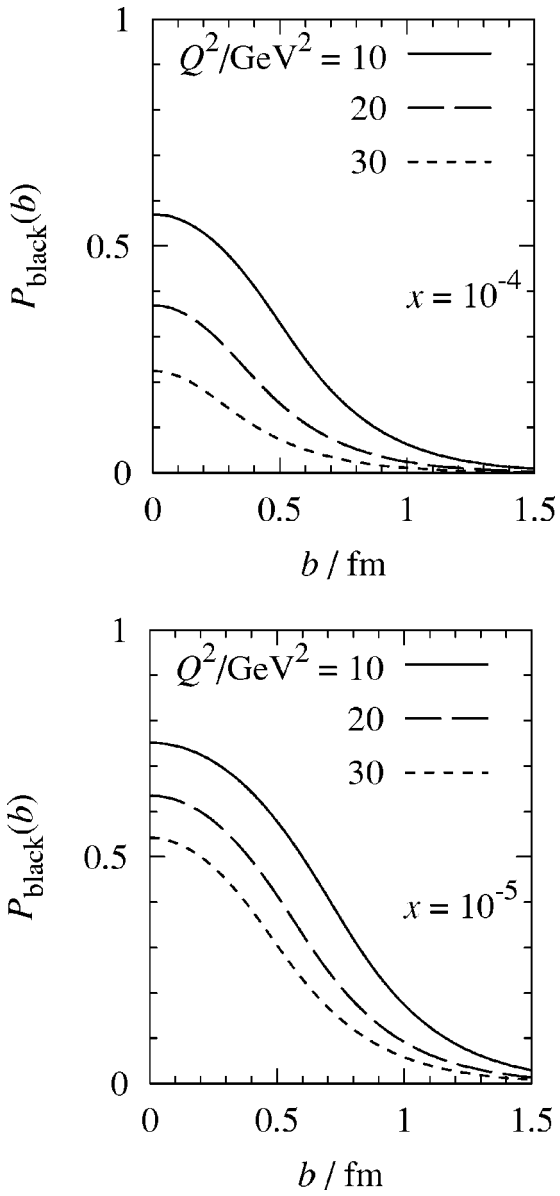

FIG. 12. The probability for partons in one proton with given x and Q^2 to interact with the other proton near the BBL, as defined by Eq. (53), as a function of the impact parameter of the proton-proton collision, b. Shown are the results for $x=10^{-4}$ (upper panel) and $x=10^{-5}$ (lower panel), for $Q^2=10$, 20 and 30 GeV^2.

Strictly speaking, the scattering of the small-x parton in one proton with the large-x_R parton in the other proton occurs at finite c.m. angles, and thus leads to a loss of light-cone fraction for the large-x_R parton. This effect should be included in a more accurate treatment.

The above results clearly show that in order to explore the BBL with partons resolved in backward or forward jets as a

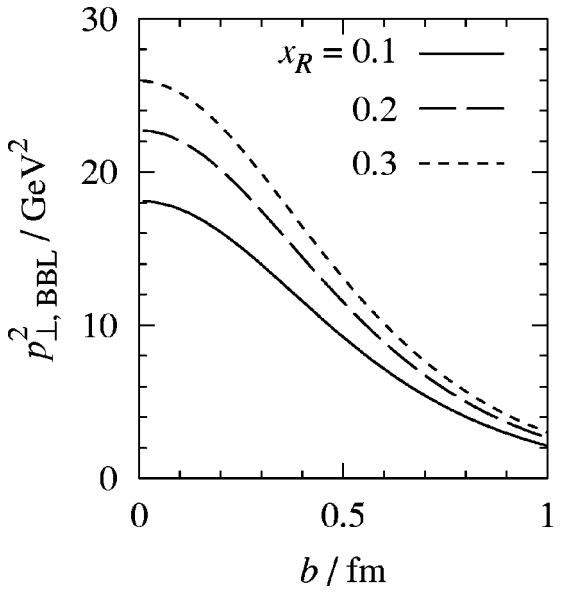

FIG. 13. The maximum value of the jet transverse momentum squared, $p^2_{\perp,\mathrm{BBL}}$, for which a small-x parton in one proton, resolved in a collision with a large-x_R parton in the other proton, interacts with the other proton close to the blackbody limit (BBL), as a function of the impact parameter of the proton-proton collision, b. The criterion for proximity to the BBL is $P_{\mathrm{black}}(b)>1/2$; see Eq. (56). Shown are the results for $x_R=0.1$, 0.2 and 0.3.

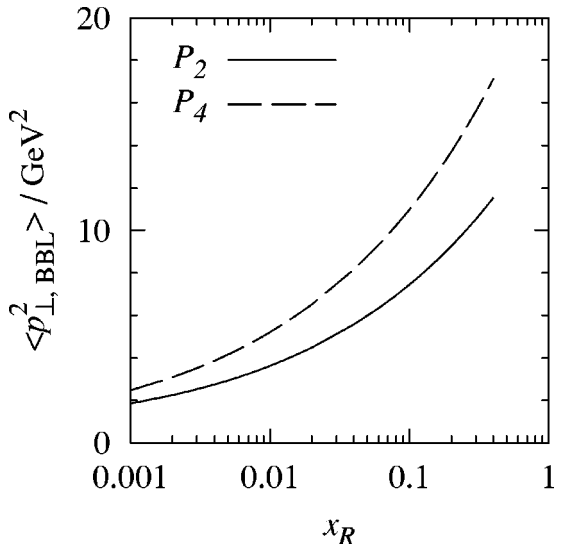

FIG. 14. The average value of $p^2_{\perp,\mathrm{BBL}}$, cf. Fig. 13, over impact parameters of the proton-proton collisions, Eq. (57), as a function of the resolving parton's momentum fraction, x_R. Shown are the averages computed with the impact parameter distribution corresponding to the hard dijet trigger, P_2 (solid line), and the double dijet trigger, P_4 (dashed line), for $\sqrt{s}=14000$ GeV and dijet momentum $p_\perp=25$ GeV, cf. Fig. 8.

probe one needs to limit the effective impact parameters in the pp collisions. Here the idea of using hard dijet production at central rapidities as a ''centrality filter,'' developed in Sec. IV, comes in. Assuming that the simultaneous production of central and forward or backward jets can be described incoherently, i.e., in a probabilistic manner, the probability for interactions near the BBL in events with hard dijet production is given by the average of the impact parameter-dependent $p_{\perp,\mathrm{BBL}}$ distribution of Fig. 13 with the effective b distribution implied by the hard dijet trigger, $P_2(b)$, see Sec. IV:

$$\langle p^2_{\perp,\mathrm{BBL}} \rangle_2 \equiv \int d^2b\, p^2_{\perp,\mathrm{BBL}}(b) P_2(b). \tag{57}$$

A similar definition applies to the double dijet trigger with b distribution $P_4(b)$. For the LHC energy, $\sqrt{s}=14000$ GeV, and a dijet trigger with momentum $p_\perp=25$ GeV, cf. Fig. 9, the average values of $p^2_{\perp,\mathrm{BBL}}$ obtained from Fig. 13 are shown in Fig. 14 (solid line) as a function of the resolving parton's momentum fraction, x_R. Also shown are the corresponding averages with a double dijet trigger with the same $p_\perp$ (dashed line). One sees that the average values of $p^2_{\perp,\mathrm{BBL}}$ are all $\gtrsim 1$ GeV^2, i.e., in the region where our assumption of resolved hard partons is well justified. What is equally important, the b distributions implied by the hard multijet trigger suppress the contributions from large impact parameters, $b \gtrsim 1$ fm, where $p^2_{\perp,\mathrm{BBL}}$ drops below ~ 1 GeV^2, meaning that the gluon density seen by the small-x partons is so low that the BBL is never reached in the region where our approximations are justified. For the above dijet trigger, the fraction of events with b so large that $p^2_{\perp,\mathrm{BBL}}(b)<1$ GeV^2 is no larger that $\sim 10\%$ for $x_R \gtrsim 0.1$; for the double dijet trigger it drops to $\sim 1\%$. In contrast, for generic inelastic events without the hard multijet trigger, the b distributions of Fig. 9 show that a significant fraction of events would involve b values for which our perturbative treatment would not be justified. In this sense, the possibility to control the effective impact parameters in the pp collisions by way of the hard multijet trigger is more than just an enhancement of otherwise well-defined contributions—it is crucial for the very applicability of the estimates presented here.

The above estimates are based on the interaction of color-octet (88) dipoles, corresponding to gluon partons, with the gluon field of the other proton. They can easily be extended to the case of color-triplet $(3\overline{3})$ dipoles, corresponding to quark partons; see Eq. (42) and after. In particular, one finds that in this case the values of $\langle p^2_{\perp,\mathrm{BBL}} \rangle$ are approximately 0.5 times the values for gluons over the range of x_R shown in Fig. 14, for both the dijet and the double dijet trigger.

It is worth noting that our estimate allows to avoid double counting due to multiple rescattering at the virtualities much smaller than the BBL. At the same time, it neglects an additional broadening due to the hard scattering at scales somewhat larger than BBL.

VI. FINAL STATE PROPERTIES FOR CENTRAL pp COLLISIONS

We have seen that the probability for partons in one proton to interact with the other proton near the BBL is greatly increased by a trigger on hard dijet production, which acts as a centrality filter. We now outline the consequences of such

interactions close to the BBL for the final state of the hadronic collision.

Generally speaking, partons propagating through a strong gluon field get transverse momenta of the order of the maximum transverse momentum for which the interaction remains black, $p_{\perp,\mathrm{BBL}}$, cf. the discussion in Refs. [26–29]. This value of transverse momentum is (approximately) related to the maximum Q^2 at which the BBL is still valid as

$$p_{\perp,\mathrm{BBL}} \approx Q_{\mathrm{BBL}}/2, \tag{58}$$

assuming that in the hard interaction a system with mass of the order of Q is produced. This relation can also be expressed as

$$p_{\perp,\mathrm{BBL}} \approx \frac{\sqrt{\lambda}}{2d} = \frac{3}{2d}, \tag{59}$$

where d is the dipole size, cf. Eq. (47). It is interesting that a similar numerical estimate follows from the uncertainty relation: Regarding d as conjugate to $p_\perp$ of the parton in the dipole one obtains $p_{\perp,\mathrm{BBL}} \approx \pi/(2d)$. Note that our definition of the BBL scale, Q_{BBL}, is different from the saturation scale Q_s of the color glass condensate picture; nevertheless the two scales are numerically comparable.

We have seen that in the central collisions selected by the ''centrality trigger'' the maximum transverse momenta squared, $p^2_{\perp,\mathrm{BBL}}$, are $\gg 1$ GeV^2; cf. Fig. 14. This allows us to describe the hadronization of these partons assuming independent fragmentation. In this approximation, the differential cross section for the semi-inclusive production of a given hadron h, characterized by its rapidity relative to the parent proton of the resolving parton, $\log z$, and transverse momentum, $k_\perp$, is given by [28]

$$z\frac{d\sigma^{pp\to hX}}{dz d^2k_\perp} = \sum_{i=q,g} \int d^2q_\perp d^2l_\perp \int_z^1 dx \frac{x}{z} \delta^{(2)}(\boldsymbol{l}_\perp + (z/x)\boldsymbol{q}_\perp - \boldsymbol{k}_\perp) f_{i/p}(x, Q^2_{\mathrm{BBL}}) D_{i/p}(z/x, l_\perp, Q^2_{\mathrm{BBL}}) c(q_\perp). \tag{60}$$

Here $f_{i/p}(x,Q^2)$ is the leading-twist parton (i = quark, gluon) distribution in the proton, $c(q_\perp)$ the transverse momentum distribution of the partons after passing through the strong gluon field, which can be estimated in various models (see, e.g., Ref. [27]), and $D_{i/h}$ the parton fragmentation function. Here we make the natural assumption, in line with the discussion above, that the small-x partons are resolved at the scale $Q^2 = Q^2_{\mathrm{BBL}}$, i.e. that the factorization scale is given by the maximal virtuality at which the interaction is close to the BBL. In Ref. [28] a similar approach was applied to particle production in central proton-nucleus collisions. We stress that the approximation of independent fragmentation is justified for sufficiently large values of z (leading hadrons); the relevant range in z grows with the transverse momentum of the produced hadrons. For small z coherence effects need to be taken into account, see Ref. [30] for a discussion.

In the BBL, estimates based on Eq. (60) should be regarded as an upper bound for the spectrum of leading particles, since in the case of large-angle scattering a parton may actually convert into two high-$p_\perp$ partons with, on average, equal light cone fractions, resulting in an even steeper drop of the leading hadron spectrum with z. This is what happens in deep-inelastic scattering of a virtual photon in the BBL [26]. In our case we expect somewhat smaller suppression due to this effect, because large impact parameters contribute to the process (although with small probability), and in this case much more forward particles would be produced. At the same time, the abovementioned trend of a steeper drop of the spectrum with z should be much more pronounced for large-$k_\perp$ particles, since in collisions at large impact parameters very few large-$k_\perp$ particles would be produced.

A detailed numerical investigation of hadron production in pp collisions based on Eq. (60) is beyond the scope of the present paper. Here we only list some expectations for the qualitative properties of hadron production at large rapidities which follow from independent fragmentation in the BBL:

(i) The leading particle spectrum will be strongly suppressed compared to interactions far from the BBL. The suppression will be especially pronounced for nucleons, so that for $z \gtrsim 0.1$ the differential multiplicity of pions should exceed that of nucleons.

(ii) The average transverse momenta of the leading particles will be $\gtrsim 1$ GeV/c.

(iii) There will typically be no correlation between the transverse momenta of leading hadrons, since they originate from two different partons which have uncorrelated transverse momenta. Some correlations will remain, however, because two partons produced in collisions of small-x and large-x partons may end up at similar rapidities.

(iv) For small impact parameters (which constitute a relatively small fraction of the total inelastic cross section but dominate in new particle production) a large fraction of the events will have no particles with $z \geqslant 0.02$–0.05. This suppression will occur simultaneously in both fragmentation regions, corresponding to the emergence of long-range rapidity correlations between the fragmentation regions. For studies of this feature of the central pp collisions it would be desirable to have good acceptance for both leading charged and neutral particles. This would allow one to measure the fraction of events without leading particles as a function of the centrality of the collision.

(v) In the forward production of dimuons or dijets one expects a broadening of the distribution over transverse momenta [31], as well as a weaker dependence of the dimuon production cross section on the dimuon mass for masses $\leqslant$ few GeV [29].

(vi) The background for heavy particle or high-$p_\perp$ jet production should contain a significant fraction of hadrons with transverse momenta $p_\perp \sim p_{\perp,\mathrm{BBL}}$, originating from frag-

mentation of partons affected by the strong gluon field. The direction of the transverse momenta of these hadrons should be unrelated to the transverse momenta of the jets. This phenomenon will make it difficult to establish the direction of jets unless $p_\perp(\text{jet}) \gg p_{\perp,\text{BBL}}$.

In connection with particle production at large rapidities, another interesting quantity to study will be the incident energy dependence of the leading particle x_F multiplicity with the dijet ''centrality trigger'' for fixed values of x_1 and x_2. In the absence of the trigger this would correspond to the study of usual Feynman scaling violations. In this case it is known that different impact parameters contribute, and that leading particle production is predominantly a large impact parameter phenomenon, which likely leads to a rather weak violation of Feyman scaling. On the other hand, in the ''conditional multiplicity'' with the centrality trigger small impact parameters give the dominant contribution, and thus the suppression of the forward spectrum should strongly increase with energy.

The proximity to the BBL in central *pp* collisions will also lead to observable effects in particle production at small rapidities. One expects a significant increase of the multiplicity at small rapidities, because interactions in the BBL will likely lead to generation of large color charges in the fragmentation regions. Also, as we discussed in Sec. IV, the production of multiple minijets will be strongly enhanced. Such an increase should in fact be present already at the Tevatron collider, in events with a trigger on two-jet or Z^0 production. We are aware of only one study [32] which investigated the correlation of the underlying event structure with the presence of such a trigger. An increase of the multiplicity at small rapidities was indeed observed.

The detailed modeling of the phenomena outlined in this section will require building a Monte Carlo event generator, accounting for the proximity of the spectator interactions to the BBL and for the new pattern of flow of color excitations.

VII. CONCLUSIONS

In this paper we have demonstrated that a trigger on hard dijet production strongly reduces the effective impact parameters in *pp* collisions at LHC and, to some extent, at Tevatron energies. The possibility to select central collisions with a reasonable rate is of considerable practical importance.

We have argued that the structure of the final states in central *pp* collisions at LHC energies will differ significantly from that of minimal bias events. The reason is that in the central transverse region the interaction of hard partons with the gluon field in the other proton approaches the unitarity (blackbody) limit, leading to an enhancement of transverse momenta and depletion of longitudinal momenta in hadron production at large rapidities.

The proposed centrality trigger offers new opportunities for realistic studies of the physics of strong gluon fields in QCD. On the experimental side, it singles out central events for which the chances of reaching the BBL are maximized, and its signatures in the final state can be clearly identified. On the theoretical side, it quantitatively defines the region in transverse space in which one should expect deviations from DGLAP evolution due to unitarity effects. This information should be incorporated in studies of nonlinear QCD evolution within the renormalization group approach; see, e.g., Ref. [33] and references therein. So far, such studies have assumed infinite extension of the ''dense gluon medium'' in the transverse plane. They have also neglected the contributions of large-x partons to the parton densities at small x due to $\log Q^2$ evolution, which are taken into account in our approach.

New heavy particles at LHC will be produced practically only in central collisions, as can be selected with the proposed hard dijet trigger. The fact that such collisions are also the ones in which the interactions of hard partons reaches the BBL poses new challenges for the analysis of such events. One needs to identify the signatures of new particle production on top of the very specific modifications of the final state implied by the BBL in the central region. This could imply, e.g., changes in the definition of jets due to the enhanced pedestal of soft hadrons and enhanced production of minijets, as well as changes in the cuts necessary to define an isolated lepton. Furthermore, the sizable ''intrinsic'' $p_\perp$ of the partons acquired from interactions with the strong gluon field may impose limits on the accuracy of the determination of the masses of produced heavy particles.

There is an interesting connection of the *pp* collisions at LHC energies discussed here with cosmic ray physics near the Greisen-Zatsepin-Kuzmin (GZK) cutoff, see Ref. [34] for a recent review. The density of gluons through which a proton propagates in central *pp* collisions at LHC energies is comparable to the typical density encountered by a proton near the GZK cutoff in collisions with air (i.e., light nuclei). Thus the BBL effects on forward particle production described above could have an impact on the energy spectrum and composition of cosmic rays near the GZK cutoff.

Learning how hadron production depends on the impact parameter of the *pp* collision will allow to address also other questions of strong interaction dynamics, not primarily related to the BBL. For example, it is often argued that events with large hadron multiplicities (a factor of $\geqslant 2$ larger than average) at small rapidities are due to collisions at small impact parameters, in which the soft parton clouds of the colliding protons overlap much stronger than in average collisions. Once the correlation between the centrality of the collision and the suppression of the forward spectra, etc., has been established with the help of the dijet trigger, one would be able to check whether similar effects are present also in the high-multiplicity events, testing the hypothesis that these are central collisions.

Finally, the comparison of our model estimate of the cross section for double dijet production with the CDF data [7] indicates that there may be significant spatial correlations of partons in the transverse plane. This interesting phenomenon should be investigated further. Not only is it important for possible extensions of the single dijet trigger to multiple dijet production—it may also reveal interesting information about the structure of the nucleon at low scales, which generates the parton distributions at the dijet production scale through Q^2 evolution.

ACKNOWLEDGMENTS

The DGLAP evolution code used in the present study has been derived from a code obtained from J. Kwiecinski several years ago. We are grateful to V. Guzey and H. Weigert for interesting theoretical discussions, and to R. D. Field for discussions related to the CDF data. L.F. acknowledges the hospitality of Penn State University. M.S. thanks the Alexander-von-Humboldt Foundation for financial support. C.W. is supported by Deutsche Forschungsgemeinschaft. This work has been supported by D.O.E.

[1] V.N. Gribov, Nucl. Phys. **22**, 249 (1961).
[2] M.M. Block and R.N. Cahn, Rev. Mod. Phys. **57**, 563 (1985).
[3] L. Frankfurt and M. Strikman, Phys. Rev. D **66**, 031502 (2002).
[4] H. Abramowicz and A. Caldwell, Rev. Mod. Phys. **71**, 1275 (1999).
[5] L. Frankfurt, V. Guzey, and M. Strikman, J. Phys. G **27**, R23 (2001).
[6] T. Sjostrand and M. van Zijl, Phys. Rev. D **36**, 2019 (1987).
[7] CDF Collaboration, F. Abe *et al.*, Phys. Rev. Lett. **79**, 584 (1997); Phys. Rev. D **56**, 3811 (1997).
[8] V.N. Gribov, hep-ph/0006158.
[9] M.M. Islam, R.J. Luddy, and A.V. Prokudin, Mod. Phys. Lett. A **18**, 743 (2003).
[10] A.B. Kaidalov, V.A. Khoze, A.D. Martin, and M.G. Ryskin, Acta Phys. Pol. B **34**, 3163 (2003).
[11] G. Alberi and G. Goggi, Phys. Rep. **74**, 1 (1981).
[12] M. Strikman and C. Weiss, hep-ph/0308191.
[13] M. Burkardt, Int. J. Mod. Phys. A **18**, 173 (2003).
[14] P. V. Pobylitsa, Phys. Rev. D **66**, 094002 (2002).
[15] ZEUS Collaboration, S. Chekanov *et al.*, Eur. Phys. J. C **24**, 345 (2002).
[16] J. Kwiecinski and D. Strozik-Kotlorz, Z. Phys. C **48**, 315 (1990).
[17] M. Gluck, E. Reya, and A. Vogt, Eur. Phys. J. C **5**, 461 (1998).
[18] FELIX Collaboration, E. Lippmaa *et al.*, SLAC-R-638; A. Ageev *et al.*, J. Phys. G **28**, R117 (2002).
[19] G. Calucci and D. Treleani, Phys. Rev. D **60**, 054023 (1999).
[20] A.H. Mueller and H. Navelet, Nucl. Phys. **B282**, 727 (1987).
[21] L. McLerran, hep-ph/0311028. E. Iancu and R. Venugopalan, hep-ph/0303204.
[22] A.H. Mueller and B. Patel, Nucl. Phys. **B425**, 471 (1994).
[23] T. Rogers, V. Guzey, M. Strikman, and X. Zu, hep-ph/0309099.
[24] B. Blaettel, G. Baym, L.L. Frankfurt, and M. Strikman, Phys. Rev. Lett. **70**, 896 (1993); B. Blaettel, G. Baym, L.L. Frankfurt, H. Heiselberg, and M. Strikman, Phys. Rev. D **47**, 2761 (1993).
[25] L. Frankfurt, G.A. Miller, and M. Strikman, Phys. Lett. B **304**, 1 (1993).
[26] L. Frankfurt, V. Guzey, M. McDermott, and M. Strikman, Phys. Rev. Lett. **87**, 192301 (2001).
[27] A. Dumitru and J. Jalilian-Marian, Phys. Rev. Lett. **89**, 022301 (2002).
[28] A. Dumitru, L. Gerland, and M. Strikman, Phys. Rev. Lett. **90**, 092301 (2003).
[29] L. Frankfurt and M. Strikman, Phys. Rev. Lett. **91**, 022301 (2003).
[30] Y.L. Dokshitzer, V.A. Khoze, S.I. Troian, and A.H. Mueller, Rev. Mod. Phys. **60**, 373 (1988).
[31] F. Gelis and J. Jalilian-Marian, Phys. Rev. D **66**, 094014 (2002).
[32] CDF Collaboration, R.D. Field, in Proceedings of the APS/DPF/DPB Summer Study on the Future of Particle Physics (Snowmass 2001), edited by N. Graf, eConf **C010630**, P501 (2001), hep-ph/0201192; CDF Collaboration, T. Affolder *et al.*, Phys. Rev. D **65**, 092002 (2002); CDF Collaboration, R. Field, Int. J. Mod. Phys. A **16S1A**, 250 (2001).
[33] K. Rummukainen and H. Weigert, hep-ph/0309306.
[34] M. Nagano and A.A. Watson, Rev. Mod. Phys. **72**, 689 (2000).